# Climate Patterns and Environmental Forces in the Mediterranean: A Neural Network Approach

Author: Massimiliano Sist[1,2], massimiliano.sist@studenti.unisalento.it
Supervisor: Prof. Piero Lionello[1]
[1]Università degli studi di Napoli "Parthenope", [2]Università del Salento

## Abstract

This study analyses the climate variability in the Mediterranean region, leveraging the capabilities of Long Short-Term Memory (LSTM) neural networks to investigate the effects of environmental forcings on temperature and precipitation patterns over land in the period 1901-2020. The Mediterranean region, characterized by its distinct climatic zones, provides an excellent opportunity to examine the heterogeneous impacts of various forcings, including carbon dioxide levels, aerosol concentrations, solar irradiance, and climatic indices. The LSTM neural network based on these forcings can successfully reconstruct the observed variability and trends of the Mediterranean land temperature (particularly at the monthly scale). Our analysis highlights the significant role of carbon dioxide as a primary driver of temperature variations across the Mediterranean, underscoring its influence across annual, seasonal, and monthly timescales. In contrast, precipitation patterns present considerable challenges being modelled by Long Short-Term Memory neural networks, reflecting their high variability and the intricate nature of their determinants. The application of this kind of networks in this context not only enhances our understanding of the Mediterranean's climate system, but also demonstrates the potential of advanced neural network models in climate science and developing more informed adaptation and mitigation strategies in the face of ongoing climate change. Our research contributes to the broader discourse on climate dynamics in the Mediterranean, providing valuable insights for future studies and policymaking efforts.

**Keywords:** Mediterranean Climate Variability, Long Short-Term Memory (LSTM) Networks, Environmental Forcing Impact, Temperature and Precipitation Patterns, Ablation Study, Neural Network Modelling in Climatology

## 1 Introduction

The Mediterranean region, characterized by its unique geographical features and climatic conditions, has long been recognized as a critical area for understanding the complexities of climate variability and change. This significance stems not only from the Mediterranean's vulnerability to climate change impacts, including temperature fluctuations and precipitation variability, but also from its role as a natural laboratory for studying the broader implications of these changes on ecosystems, water resources, agriculture, and human societies (Alì et al, 2022). Amidst this backdrop, the scientific community has intensified efforts to unravel the complex mechanisms driving climate variability in the Mediterranean, focusing on the influence of environmental forcings such as carbon dioxide (CO2) levels, aerosol concentrations, climatic indices, and solar irradiance (e.g. Lionello., 2012; Cherif et al., 2021).

The Mediterranean's diverse climatic responses to environmental forcings can be further understood by recognizing its subdivision into three distinct latitudinal ranges, defined by longitudinal coordinates between 10°W and 35°E and latitudinal coordinates between 29°N and 45°N (Figure 1). This subdivision provides a nuanced framework for capturing the heterogeneous nature of climate variability at subregional scale. The Northern Mediterranean, extending from the northern coastlines to 43.5°N latitude, is characterized by temperate influences and includes regions such as the northern parts of the Iberian Peninsula, Southern France, and parts of the Balkans. It is markedly distinct from the warmer Central zone, which extends from 37.1°N down to the southern coastlines, encompassing areas like the Central Mediterranean and parts of Anatolia. The Southern Mediterranean, reaching towards the northern borders of the Sahara and including regions such as the Western and Eastern Maghreb and the Levant, experiences more arid conditions and extends from 29°N up to 37.1°N. This detailed zonal approach enhances our understanding of the differential impacts of CO2 levels, aerosol concentrations, climatic indices, and solar irradiance across these climatic zones, providing insights into the region's climate system dynamics. This subdivision is not merely a geographical delineation but serves as a critical variable in the climatic analysis, offering insights into the differential impacts of CO2 levels, aerosol concentrations, climatic indices, and solar irradiance across these climatic zones. By integrating this zonal approach into our Long Short-Term Memory (LSTM) network model, we aim to enhance the resolution and relevance of our findings, thereby providing a more detailed and regionally specific understanding of climatic changes within the Mediterranean basin.

LSTM networks, a class of artificial neural networks, have emerged as a powerful tool in the analysis of temporal sequences and are particularly adept at modelling long-term dependencies in complex datasets (Emmert-Streib et al., 2020). Their capability to learn from sequences of data makes LSTM networks an ideal candidate for exploring the dynamics of climate systems, where the relationships between variables are not only nonlinear but also exhibit variability across multiple time scales. This research endeavour aims to leverage the potential of LSTM networks to dissect the impact of various forcing variables on temperature and precipitation patterns in the continental Mediterranean region over the period 1901-2020.

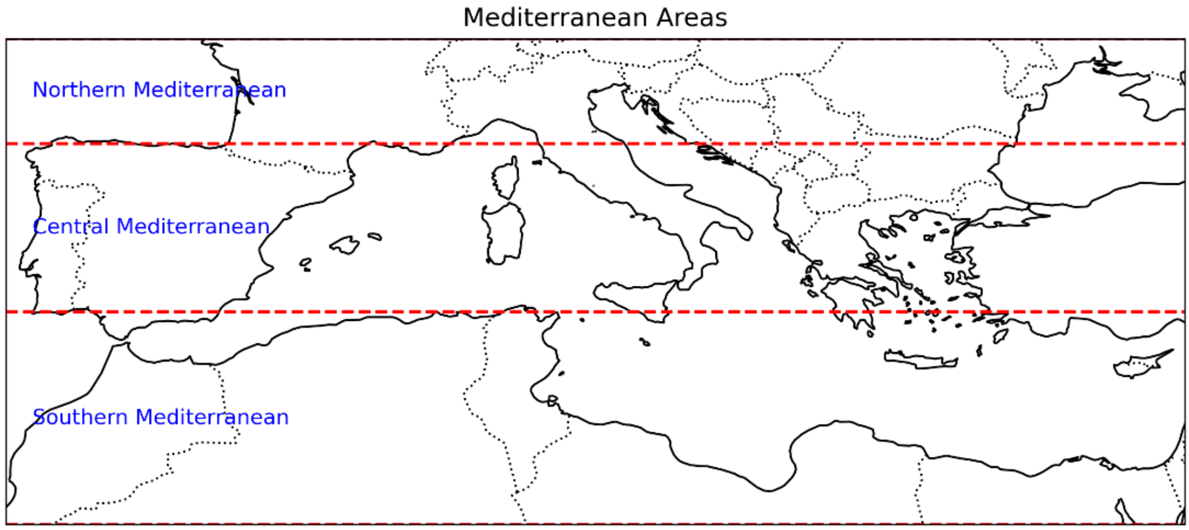


*Figure 1. Map of the Mediterranean region highlighting three key areas: Northern Mediterranean (43.5°N-47.5°N), Central Mediterranean (37.1°N - 43.5°N) and Southern Mediterranean (29°N-37.1°N)*

The study of temperature and precipitation variations in the Mediterranean is of paramount importance due to the region's sensitivity to climatic changes. The identification of the Mediterranean as a climate change 'hot spot', characterised by pronounced warming and reduced precipitation, underlines the urgency of deepening our understanding of regional climate dynamics and their responses to various environmental factors (Lionello and Scarascia, 2018).

The Mediterranean climate, characterized by hot, dry summers and mild, wet winters, is subject to significant variations that can profoundly affect the region's water availability, biodiversity, agriculture, and human well-being. Understanding the drivers behind these variations is crucial for developing effective adaptation and mitigation strategies in response to ongoing and future climatic changes.

Understanding the historic trends of temperature and precipitation in the Mediterranean region is pivotal to appreciating the present climate dynamics and anticipating future changes. The following figures illustrate the annual trends in temperature and precipitation across the Northern, Central, and Southern Mediterranean zones from 1901 to 2020, underscoring the region's susceptibility to climatic fluctuations and the profound impacts of environmental forcings.

Figure 2 shows the annual temperature trend for each Mediterranean zone. A clear warming trend is evident, with temperatures rising over the past century, reflecting global patterns of climate change and regional responses to increasing greenhouse gas concentrations.

Figure 3 depicts the annual precipitation trend within the same zones. Here, the variability and complexity of precipitation patterns are apparent, with notable fluctuations that pose challenges for accurate modelling and prediction. These patterns are crucial for understanding the Mediterranean's water resources and their sustainable management in the face of climate change.

The observed trends provide a backdrop for the questions this thesis seeks to answer, guiding our exploration of the intricate relationships between climate variables and the environmental forcings that influence them.

In recent years, LSTM networks have gained prominence in climatic studies for their ability to capture the temporal dynamics of environmental data. Unlike traditional machine learning models, LSTM networks can remember information over long periods, making them particularly suitable for analysing climate data, where the influence of past events can persist and influence future conditions. This capability allows for a more nuanced understanding of the temporal relationships between environmental forcings and climatic responses, providing insights into the underlying mechanisms of climate variability and change.

This study sets out to explore the use of LSTM networks in analysing and understanding the impact of 'forcing variables' on temperature and precipitation variations in the continental Mediterranean region.

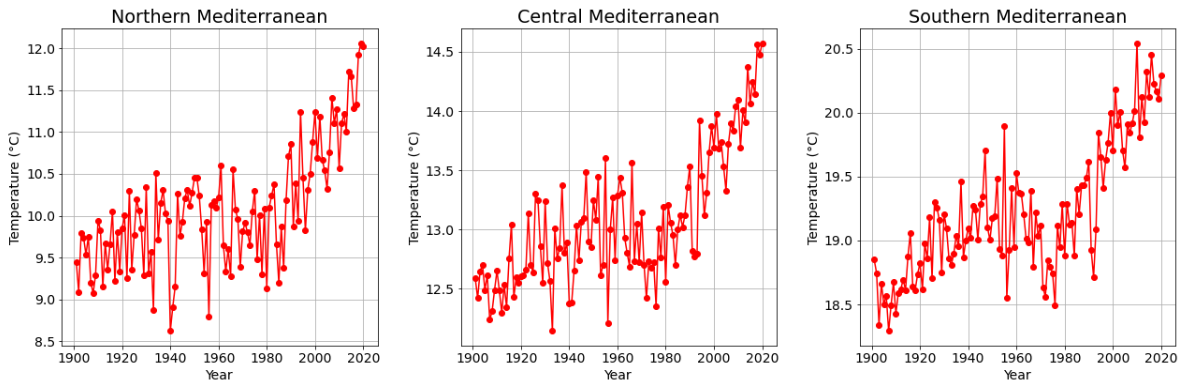


*Figure 2. Annual temperature trends in the three reference areas*

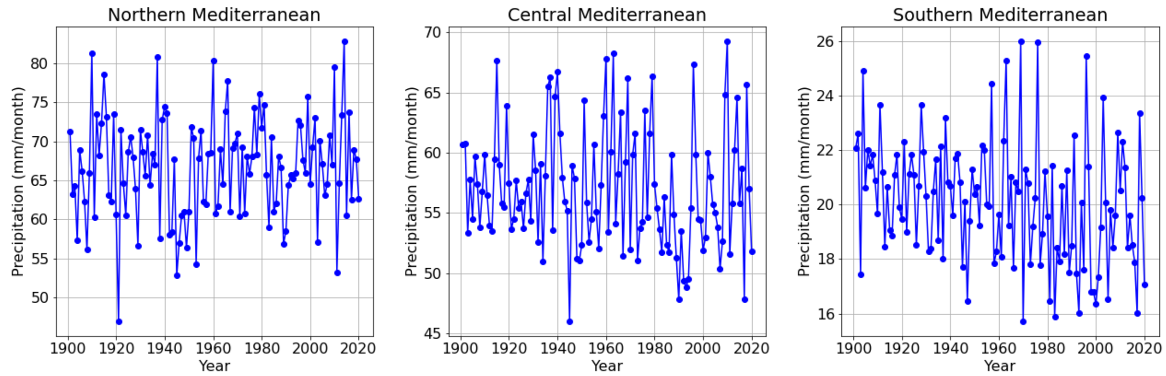


*Figure 3. Annual rainfall trends in the three reference areas*

By integrating LSTM models with comprehensive datasets on CO2 levels, aerosol concentrations, climatic indices, and solar irradiance, this study aims to unravel the complex interactions between forcing variables and climate outcomes. Specifically, the research seeks to answer the following questions:

- How do variations in CO2 levels and aerosol (both anthropogenic and natural, including volcanic) concentrations influence temperature and precipitation patterns in the continental Mediterranean region?
- What role do climatic indices large scale processes external to the Mediterranean region (e.g., North Atlantic Oscillation, Atlantic Meridional Overturning Circulation, El Niño-Southern Oscillation) play in modulating temperature and precipitation variability in this region?

- To what extent does solar irradiance contribute to the observed climatic changes over the study period?

By addressing these questions, this thesis aims to contribute to the broader understanding of climate dynamics in the Mediterranean region. Furthermore, it seeks to demonstrate the potential of LSTM networks as a valuable tool for climate research, offering new perspectives on the analysis of climatic data and the prediction of future climate scenarios. Through this investigation, we aspire to enhance our comprehension of the Mediterranean climate system, paving the way for informed decision-making in the face of climatic uncertainties.

## 1.1 Background and Literature Review

The Mediterranean region, characterized by its unique climatic patterns, has been the subject of extensive research due to its sensitivity to climate variability and change. Recent studies (Pappas et al., 2021, Li et al., 2020) have increasingly focused on the analysis of climatic variations using advanced computational models, with a particular emphasis on the application of neural networks. This chapter provides an overview of the current knowledge on climate variations in the Mediterranean and reviews the literature on Long Short-Term Memory neural networks, highlighting their applications in climatological and environmental fields. It also discusses the impact of CO2, aerosols, climatic indices, and solar irradiance on the Mediterranean climate.

The Mediterranean climate is influenced by a variety of environmental forcings, such as changes in atmospheric composition, land-use modifications, and variations in solar activity (Lionello et al., 2006). The research conducted by Pasini et al. is pivotal in examining the dynamics between various forcings and temperature across different scales of the climate system, highlighting the significant impact of anthropogenic factors on recent temperature trends as shown in their 2006 study (Pasini et al., 2006). Their further application of neural network methodologies in 2017 (Pasini et al., 2006) deepens our understanding of the intricate contributions of human activities, notably greenhouse gas and aerosol emissions, to global and regional climate alterations. These insights reflect the utility of advanced analytical approaches, like neural networks, in broadening the scope of climate change research beyond traditional methods.

## 1.2 LSTM Neural Networks in Climatology

The advent of LSTM neural networks has opened new avenues for analysing and predicting climatic variables. LSTM networks, known for their ability to learn from sequences of data over long periods, have proven to be particularly useful in modelling complex climatic systems where the influence of past events can extend far into the future. Recent applications of LSTM networks in climatology include sea surface temperature prediction (Hou, Siyun, et al., 2021), soil moisture and temperature prediction (Li, Qingliang, et al., 2022), and the assessment of climate change effects on dust activity (Hamidi, M., & Roshani, A., 2023). These studies demonstrate the versatility of LSTM networks in capturing the non-linear dynamics of climatic processes and their potential for enhancing our understanding of climate variability and change.

For instance, the study "Prediction of 3-D Ocean Temperature by Multilayer Convolutional LSTM" (Zhang, et al., 2020) presents an innovative approach to predicting ocean temperatures at various depths, highlighting the importance of subsurface temperature in understanding ocean dynamics. This research exemplifies the application of LSTM networks in capturing both horizontal and vertical temperature variations, providing valuable insights into the complex interactions within the oceanic component of the climate system.

## 1.3 Impact of Environmental Forcings on the Mediterranean Climate

The Mediterranean climate is influenced by various environmental forcings, including CO2 concentrations, aerosols, climatic indices (e.g., North Atlantic Oscillation, El Niño-Southern Oscillation), and solar irradiance. Many studies underscore the complex interplay between these forcings and the Mediterranean climate (Lionello et al., 2006). Neural Networks have already been used to show the effects of aerosol concentrations and solar irradiance on precipitation patterns and temperature regimes in the Mediterranean region (Pasini et al., 2006). Moreover, the analysis of climate change effects on Iraq dust activity using LSTM (Hamidi, M., & Roshani, A., 2023) illustrates how regional climatic variations, driven by environmental forcings, can have broader implications for air quality and public health. This underscores the importance of understanding the specific impacts of different forcings on the Mediterranean climate to inform mitigation and adaptation strategies.

## 2 Data and methods

Before delving into the specifics of our Long Short-Term Memory (LSTM) model implementation for climate study, it's crucial to understand the foundational principles of LSTM networks and how they operate. A feedforward neural network is a basic form of artificial neural network where the information moves in only one direction—from input nodes, through hidden layers, to output nodes, without cycles or loops. In these networks, each neuron in one layer has a weighted connection to neurons in the subsequent layer, and the final output is derived from a series of transformations that apply these weights to the input data.

In contrast, Long Short-Term Memory (LSTM) networks, as illustrated in Figure 4, belong to a more complex type of networks known as recurrent neural networks (RNNs), which are designed to handle sequential data. Unlike feedforward networks, LSTMs can maintain information in 'memory' for long periods, which is crucial for tasks that require knowledge of previous events, such as climate data analysis. Indeed, a key parameter in preparing the input sequences for the network is the 'time step'. A time step in an LSTM network refers to the number of intervals the network looks back to learn from past data to predict future outcomes.

The diagram highlights the key components of an LSTM unit:

- 'A' represents the memory cell that stores values over arbitrary time intervals.
- The input gate (σ), positioned on the left-hand side within each LSTM block, decides the extent to which new information from the current input $X_t$ should be stored in the cell state.
- The forget gate (σ), located below the input gate, determines which parts of the existing memory should be discarded.
- The output gate (σ), found on the right-hand side, regulates the contribution of the memory cell to the output at time $h_t$
- The $tanh$ function prepares the cell state for output by scaling the values, facilitating the regulation of information flow within the network.

These gates, depicted as yellow boxes and controlled by $sigmoid$ (σ) and $tanh$ functions, collectively decide at each step what information is retained or removed, based on the current input, the previous output, and the past cell state. They ensure the network's ability to capture dependencies from long ago, which is indispensable for understanding complex systems like the climate.

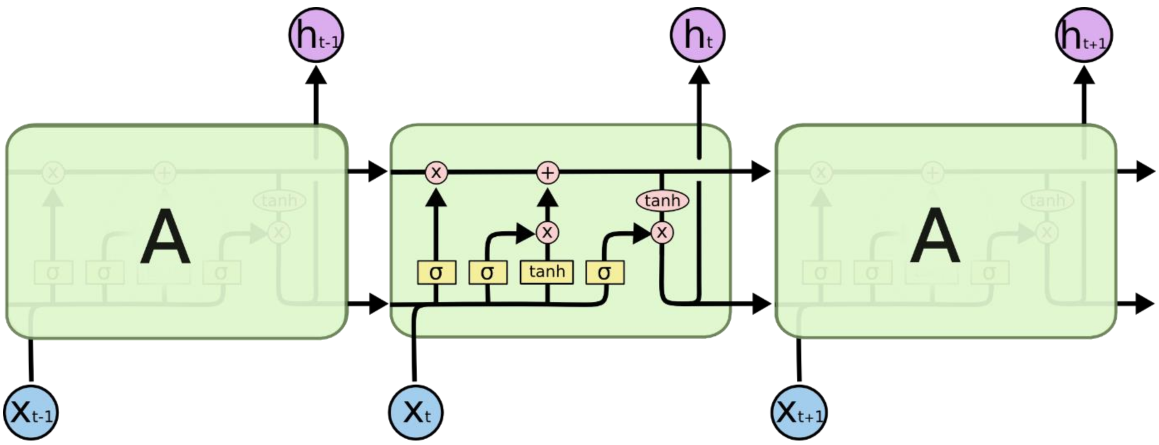


*Figure 4. A schematic of an LSTM unit, illustrating the cell state ('A'), the flow of input Xt, and output ht, alongside the recurrent connections at each time step. Sigmoid functions (σ) regulate the input and forget gates, determining the flow and modification of information, while hyperbolic tangent functions (tanh) manage the memory cell's transformation of data. This configuration allows the network to maintain essential information over long sequences.*

While a feedforward network simply maps input to output, an LSTM network does so while also considering the sequence's history.

Climate variables exhibit complex temporal dynamics, wherein past events can significantly influence future conditions over diverse timescales. LSTM networks, with their long-term memory capacity and their proficiency in modelling nonlinear relationships, are uniquely suited for capturing these dynamics, offering a potent tool for comprehending and forecasting climate variability.

Whereas feedforward networks are efficacious in modelling static and non-sequential relationships, LSTM networks excel in the processing of complex sequential data, thanks to their sophisticated structure that facilitates the tracking of information over time. This characteristic renders them ideal for applications necessitating an understanding of lengthy and intricate temporal dependencies, as is the case in climate studies.

## 2.1 Long Short-Term Memory network preparation

The preprocessing of data is a critical step in preparing inputs for the LSTM network. Our data consists of a comprehensive suite of forcing variables including CO2 concentrations, Stratospheric Aerosol optical depth, Total Solar Irradiance (TSI), and climate indices such as the North Atlantic Oscillation (NAO), Southern Oscillation Index (SOI), and Atlantic Multidecadal Oscillation (AMO). Prior to inputting into the LSTM, the datasets undergo several preprocessing stages:

- **Integration**: Multiple data sources are combined to create a comprehensive feature set. Each dataset's temporal resolution is matched to ensure consistency.
- **Normalization**: The data is normalized using the MinMaxScaler to adjust into a common scale, usually between 0 and 1, allowing the LSTM model to efficiently process the inputs without bias towards any particular scale of data.
- **Sequence Creation**: The time-series data is converted into sequences that the LSTM can process.

Each sequence contains information from past time steps to predict the next time step's outcome.

For the implementation of our LSTM model, we employ a Sequential model from the TensorFlow Keras library, which allows us to stack layers in a linear fashion. The model consists of LSTM layers followed by a fully connected Dense layer. Our architecture is composed of an initial LSTM layer with 60 neurons, an empirically determined configuration balancing complexity and computational efficiency. In defining the optimal architecture for our LSTM network, we adopted a methodical experimental approach. This involved iteratively fine-tuning the architecture by adjusting the number of layers, the number of nodes per layer, and particularly the duration of time steps, focusing on optimizing the model's performance. Through this experimental tuning, the best time step was determined to be 4 years for all temporal resolutions of the dataset used. The relu activation function is utilized for its proficiency in handling non-linear data and mitigating the vanishing gradient problem. This is followed by a Dense output layer with a single neuron to predict the target variable, which in this case is either temperature or precipitation. The model is compiled using the Adam optimizer and Mean Squared Error loss function, providing robustness against outliers and ensuring the convergence of gradients during training.

To facilitate the training process, we divided the dataset into a training set and a testing set, allocating 20% of the data for testing, consistent with standard practices in machine learning. This partition was executed using the Python command:

$$train\_test\_split(x\_seq, y\_seq, test\_size = 0.2, random\_state = 42),$$

ensuring a random yet reproducible selection of the 20% of data as the test set. Setting the random_state parameter guarantees the reproducibility of our data selection, a crucial factor for experimental validity. This methodology allows the model to be assessed on a dataset not encountered during the training phase, offering a more reliable measure of its generalization capability.

To prevent overfitting and ensure that training ceases once the model's performance on a validation set no longer shows improvement, we utilized the EarlyStopping callback. Performance evaluation was conducted using the Mean Squared Error (MSE) and Mean Absolute Error (MAE) metrics, comparing the model's predictions with actual observations in the test set.

## 2.2 Multi-Temporal average data

To conduct a thorough analysis of the climatic trends across different time scales within the Mediterranean region, it was essential to transform our original datasets, which were based on monthly averages, into a format conducive to multi-temporal analysis. This section elucidates the methodologies employed for aggregating the monthly data into seasonal and annual averages, alongside maintaining their original monthly format for a granular temporal analysis. This reformatting is pivotal for capturing the nuanced climatic dynamics across the Mediterranean and offers a comprehensive framework for examining temperature and precipitation variabilities on monthly, seasonal, and annual bases.

- **Monthly Averages:** The primary dataset, inherently structured as monthly averages, was utilized directly to assess the short-term climatic fluctuations within each year, providing insight into the intra-annual variabilities of temperature and precipitation.
- **Seasonal Averages:** the seasonal averages were computed by first mapping each month of our dataset to its corresponding meteorological season: Winter (December to February), Spring (March to May), Summer (June to August), and Autumn (September to November). We then calculated the mean of the climatic measurements for each of these seasonal groupings. This method provided a clearer view of the climate's rhythmic changes throughout the year, allowing us to pinpoint and analyse specific trends and variations inherent to each season.
- **Annual Averages:** The annual averages were derived by aggregating the data over each calendar year, thus allowing us to analyse the broader, long-term climate trends and assess how temperature and precipitation have varied on an annual scale over the study period.

This detailed data aggregation process was instrumental in enabling a multi-scaled analysis of climate variability, enhancing the depth of our understanding of the climatic changes occurring within the Mediterranean region.

## 2.3 Dataset Description

In this study, an array of datasets encompassing a range of climatic and environmental parameters was compiled.

- The Climatic Research Unit Time Series (CRU TS v. 4.04) dataset for temperature, offering a spatial resolution of 0.5° by 0.5° latitude/longitude and extending from 1901 through 2020 (Harris et al. 2020).
- The Global Precipitation Climatology Centre's (GPCC) dataset, which offers a similar spatial resolution (Schneider et al., 2022).
- CO2 concentrations data derived from the North American Carbon Program (Wei et al., 2014), providing a granular global atmospheric carbon dataset crucial for carbon cycle modelling.
- Stratospheric Aerosol Loading data, obtained from the Goddard Institute for Space Studies, presenting vital aerosol optical depth estimations since the 1850s (Sato et al., 1993).
- Total Solar Irradiance (TSI), essential for climate change studies due to their impact on Earth's radiative balance (Lean et al., 1995).
- The Southern Oscillation Index (Ropelewski et al., 1987)
- The North Atlantic Oscillation (Allan et al., 1991)
- The Atlantic Multidecadal Oscillation (Compo et al., 2011, Enfield et al., 2017),

The datasets have been rigorously verified for completeness and processed with advanced statistical techniques to uphold the integrity of our climatic analysis. Each dataset, enriched with historical breadth, contributes to a nuanced understanding of climate variability, which is fundamental for projecting future climatic conditions in the Mediterranean basin.

## 2.4 Score And Statistics

### 2.4.1 Performance

The efficacy of LSTM networks has been rigorously assessed for the climatic divisions of the Mediterranean - Northern, Central, and Southern zones. These advanced models were evaluated for their predictive prowess in both temperature and precipitation across annual, monthly, and seasonal data

scales. The analysis was anchored on the coefficient of determination $R^2$ and Relative MAE Error, both pivotal metrics in climatology for model accuracy evaluation.
The coefficient of determination $R^2$, quantifies the proportion of variance in the dependent variable that is predictable from the independent variable(s). It provides a measure of how well observed outcomes are replicated by the model, based on a normalized scale from 0 to 1. A value of $R^2$ closer to 1 indicates a strong correlation and significant predictive capability. Mathematically, $R^2$ is defined as:

$$R^2 = 1 - \frac{\sum_{i=1}^{n}(y_i - \hat{y}_i)^2}{\sum_{i=1}^{n}(y_i - \bar{y})^2}$$

where $y_i$ are the actual values, $\hat{y}_i$ are the values predicted by the model, and $\bar{y}$ is the mean of the actual values.
The Relative MAE Error, on the other hand, relates the Mean Absolute Error (MAE) to the Mean Absolute Deviation (MAD) of the actual values, thereby providing a normalized measure of errors that accounts for the dispersion of the data. A lower value indicates that the model has errors that are minor relative to the inherent variability of the data. The Relative MAE Error is given by the ratio:

$$Relative\ MAE\ Error = \frac{MAE}{MAD}$$

Where MAD and MAE are calculated as:

$$MAD = \frac{1}{n}\sum_{i=1}^{n}|y_i - \bar{y}|$$

$$MAE = \frac{1}{n}\sum_{i=1}^{n}|y_i - \hat{y}_i|$$

In this investigation, these metrics serve as the primary supports for assessing model efficacy, enabling us to dissect the LSTM network's ability to simulate climate phenomena with respect to the diverse temporal and spatial climatology of the Mediterranean region.

### 2.4.2 Ablation

Following the establishment of our LSTM model, an ablation study was undertaken to discern the influence of individual forcing variables, on the model's predictive accuracy. This was achieved by systematically modifying specific input variables within the test dataset to their mean values across the dataset. This method simulates the absence of specific influences of these variables without altering the architecture or weights of the LSTM model, a process known as 'feature ablation.'
To quantify the impact of each ablated forcing variable, we employed a metric termed Score Difference, which is calculated as follows:

$$ScoreDifference = Performance_{ablated} - Performance_{original}$$

where $Performance_{original}$ is the model's loss score evaluated with all forcing variables included, and $Performance_{ablated}$ is the loss score evaluated with one of the forcing variables set to its mean value and the loss score is simply the Mean Squared Error (MSE) defined as:

$$MSE = \frac{1}{n}\sum_{i=1}^{n}(y_i - \hat{y}_i)^2$$

This score specifically refers to the loss function value returned by the $model.evaluate()$ method in TensorFlow, which measures the model's prediction error; a lower score indicates better model performance. Thus, a positive ScoreDifference signifies that the removal (or modification to the mean) of the feature has resulted in increased prediction error, underscoring the importance of that feature in the model's predictions.

This ablation process enables us to unravel the individual and collective significance of environmental forcing variables in the LSTM network's ability to reconstruct climatic trends, thereby providing a more granular understanding of the model's inner workings and the complex interplay among climatic drivers. To further enhance the comprehensiveness of our analysis, it's important to note that the entirety of the dataset was utilized for specific visual representations and ablation tests. This approach allowed us to generate a complete view of the model's capabilities across all available data, enriching our understanding of its performance and the impact of forcings on Mediterranean climate variability. This distinction between the training/testing split and the use of the complete dataset for certain analyses is crucial for a nuanced interpretation of our results.

# 3 Results

Before delving into the detailed results obtained from the testing dataset, we highlight that some of the analyses, including visual representations in figures such as Figure 5 and ablation studies, were conducted using the full dataset. This methodological choice was made to capture the model's broader applicability and to deeply investigate the influence of various input features on climate predictions.

The detailed quantitative analysis of our LSTM models, specifically the $R^2$ and Relative Mean Absolute Error metrics that demonstrate their predictive performance, can be thoroughly reviewed in Table 1 and in Table 2 in the Appendix.

For an in-depth understanding of the influence of various forcing variables on our models, the numerical values derived from our ablation studies are tabulated in Table 3 and Table 4 in the Appendix.

## 3.1 Annual Reconstruction Performance

Evaluating the annual performance of LSTM networks for reconstructing precipitation and temperature across the different Mediterranean zones yielded nuanced insights into the models' capabilities.

The $R^2$ (Figure 7) and Relative Mean Absolute Error (Rel. MAE) (Figure 8) were instrumental in assessing model performance with a keen focus on their interpretability and implications for climatic modelling.

In the Central zone, the LSTM model for annual precipitation demonstrated an $R^2$ of -0.034 (Figure 7), hinting at challenges in accurately modelling precipitation cycles. The Rel. MAE was 0.870 (Figure 8), suggesting that its average error is within the limits the typical data variability. This is visually underscored in Figure 6, which compares the actual monthly precipitation values with those reconstructed by the LSTM model over time. The visual representation starkly demonstrates the LSTM model's limitation in capturing the variability of precipitation patterns. While the reconstructed values—indicated by the red line—generally follow the mean trajectory of the actual data, shown in blue, they fail to replicate the variability and the peaks and troughs characteristic of the precipitation measurements. This discrepancy highlights the model's tendency to smooth out the data, capturing only the general trend rather than the precise fluctuations over time.

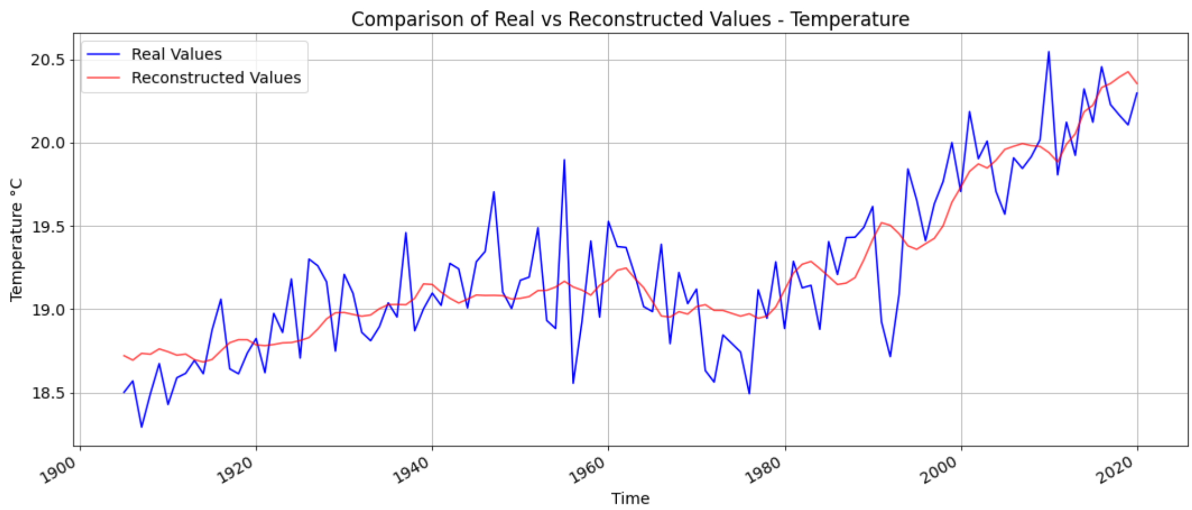


*Figure 5. Reconstructed vs. Actual annual mean temperature in the Southern Mediterranean: This graph showcases the LSTM network's ability to accurately model rising temperature patterns over time, mirroring the observed warming trend in the region and highlighting the model's proficiency in climate trend analysis.*

Conversely, the model's performance in temperature prediction was more promising with an $R^2$ of 0.517, indicating that over half of the variance in temperature data could be accounted for by the model. A Rel. MAE of 0.729 for the Central zone's temperature further reflects the model's competence in this aspect, with errors small in comparison to the overall data variability (Figure 8).

In the Northern and Southern zones, similar patterns were observed. The Northern zone's annual precipitation model had a slightly positive $R^2$ of 0.011 and a Rel. MAE of 0.839, while the Southern zone exhibited an $R^2$ of -0.892, which was significantly lower, and a Rel. MAE of 0.792. These figures indicate a disparity in the model's ability to generalize across the zones, with particular difficulty in the Southern zone where the model was less effective in capturing the variance.

For temperature, the Northern and Southern zones showed $R^2$ values of 0.549 and 0.680 respectively, revealing a stronger predictive performance. The Rel. MAEs were 0.786 and 0.592, underscoring that the model's temperature predictions were relatively close to the actual data, especially in the Southern zone, which presented the lowest error relative to variability. The competence in temperature reconstruction is visually corroborated by Figure 5, which displays the LSTM model's aptitude in tracing the incremental trend of temperature over the years though missing the observed interannual variability.

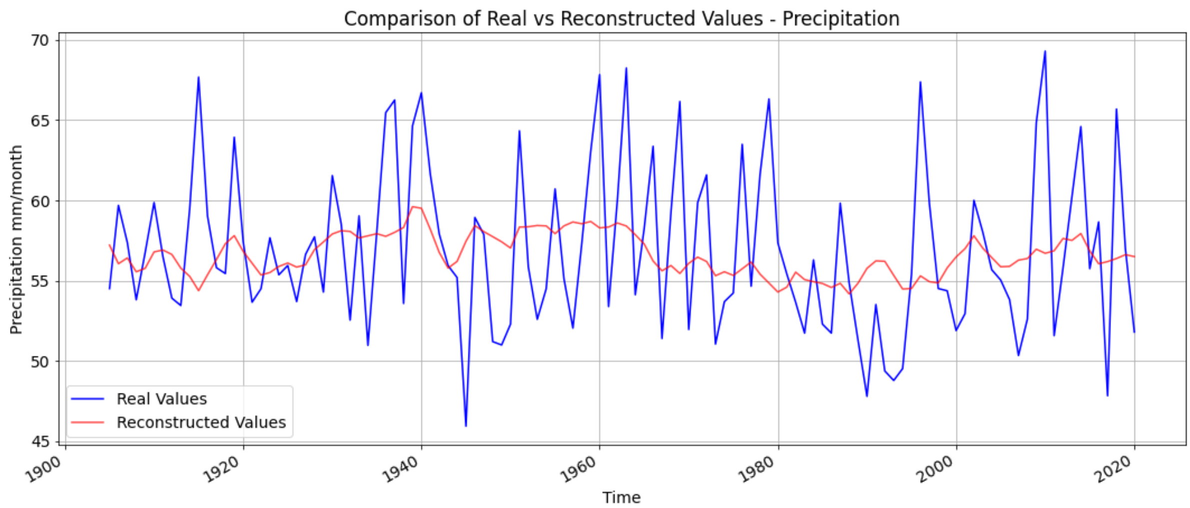


*Figure 6. Reconstructed vs. Actual annual precipitation in the Central Mediterranean: The graph illustrates the challenges faced by the LSTM network in accurately capturing the high variability of precipitation patterns. While the reconstructed values trace the general mean of actual precipitation data, they significantly smooth out the extreme fluctuations, underscoring a need for model refinement in capturing the complexity of precipitation dynamics in climate analysis.*

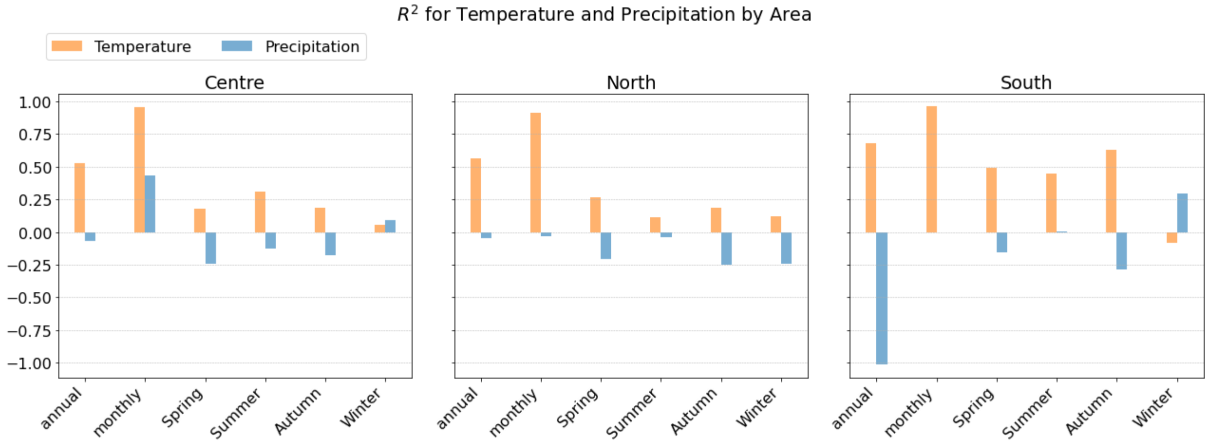


*Figure 7. "Comparative visualization of $R^2$ values for temperature and precipitation models across different regions and time periods, showcasing the variance explained by each model in the context of climate data analysis.*

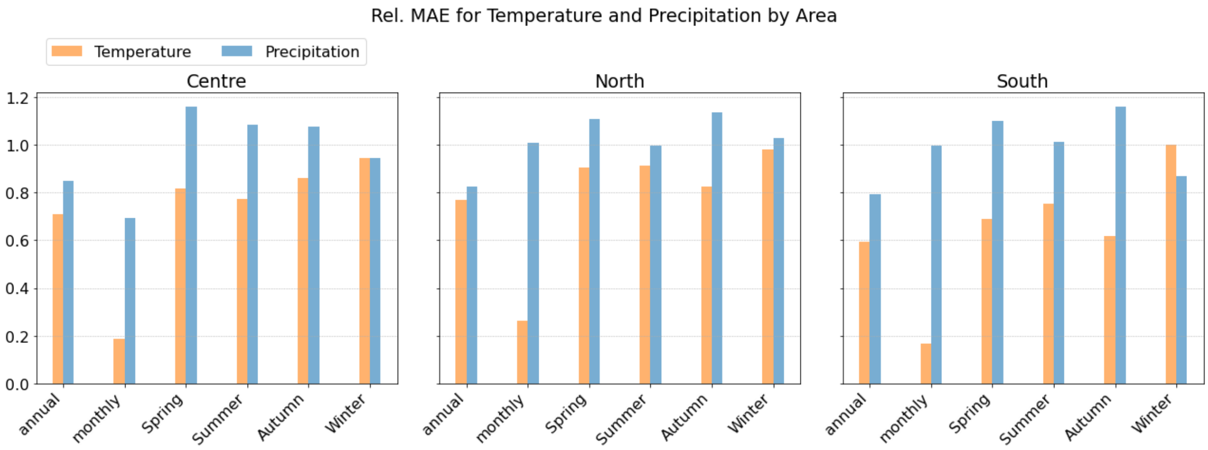


*Figure 8. Comparative visualization of Relative Mean Absolute Error (Rel. MAE) for temperature and precipitation models, reflecting the average prediction accuracy across various regions and seasonal periods within the scope of climate data analysis.*

## 3.2 Monthly Reconstruction Performance

For the Central Mediterranean zone, the LSTM models displayed a remarkable adeptness in temperature reconstruction, achieving an $R^2$ of 0.958, suggesting a strong correlation with the actual temperature values. The Rel. MAE for this region stood at 0.173, indicating the errors made by the model were minimal in relation to the variability of the actual data. This proficiency in capturing temperature trends is vividly demonstrated in Figure 9, where a smoothed comparison of real versus reconstructed monthly mean temperatures (using a 12-month moving average) highlights the LSTM model's precision. The graph summarises the model's ability to track the actual temperature trend without the clutter of individual monthly fluctuations, showcasing the accurate reconstruction capabilities for the region and emphasizing the LSTM's effectiveness in climate trend analysis.

Conversely, the reconstruction of precipitation posed a greater challenge. In the Northern zone, the LSTM models grappled with capturing the variability, reflected in a negative $R^2$ value of -0.019, which denotes that the model's predictive capability was slightly below the baseline of the mean model. This was further reinforced by a Rel. MAE close to 1, signalling that the errors were commensurate with the actual data's dispersion, thereby implying low predictive reliability for precipitation in this particular setting.

The Southern zone captured a more promising picture for temperature reconstruction, with an $R^2$ of 0.934, indicative of the model's robust alignment with the actual temperature trends. The model's precision was accentuated by a Rel. MAE of 0.226, reflecting smaller deviations from the observed data when compared to the central tendency.

These findings combine to form a comprehensive understanding of the LSTM network's reconstructive skill set over a monthly scale, showcasing its strengths in discerning temperature patterns while concurrently highlighting the areas where precipitation reconstruction requires further refinement. The relative success in temperature reconstruction across all zones suggests an intrinsic capacity of the LSTM models to encapsulate the underlying temporal patterns governing temperature variations. In contrast, the heightened Rel. MAEs for precipitation underscore the inherent complexity of hydrological cycles and their manifestation in precipitation data.

The monthly scale offers a lens into the nuanced behaviour of climate variables, and the LSTM's performance herein lays bare the multifaceted nature of environmental data reconstruction. While temperature data lend themselves more readily to LSTM-based reconstruction, the heterogeneity and stochastic elements intrinsic to precipitation ensure it remains an area ripe for ongoing research and model development.

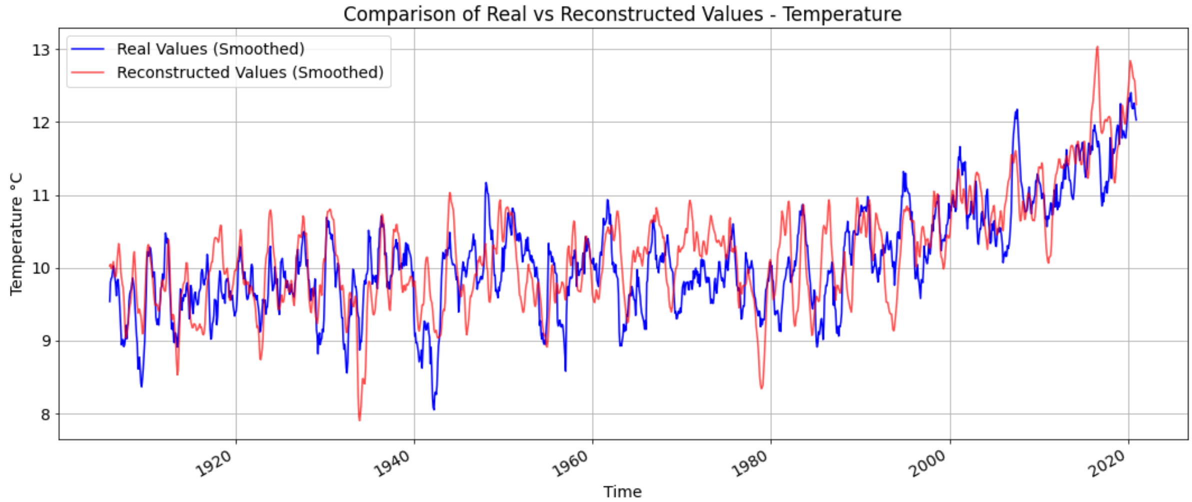


*Figure 9. Smoothed Real vs. Monthly Mean Temperature Values in the Northern Mediterranean: This graph illustrates the exceptional predictive performance of the LSTM model with a moving average applied to monthly data for clarity. The moving average, using a 12-month window, highlights the model's ability to track the actual temperature trend without the clutter of individual monthly fluctuations, showcasing the accurate reconstruction capabilities for the region.*

## 3.3 Seasonal Reconstruction Performance

In the Central zone during Autumn, the models faced significant challenges, as evidenced by a negative $R^2$ value of -0.257, which indicates that the models were unable to capture the seasonal variability effectively. This difficulty in modelling is supported by a Rel. MAE greater than 1, suggesting that the model's errors are more pronounced than the natural variability of the data.

Winter presented a contrasting scenario, with the LSTM models for the Southern zone yielding an $R^2$ Squared of 0.295, reflecting a moderate ability to reconstruct the seasonal precipitation patterns. The Rel. MAE of 0.849 for this region implies that the reconstruction errors are relatively lower than the seasonal data variability, hinting at a decent model performance in capturing the winter precipitation dynamics.

For temperature, the LSTM models performed with more consistency across seasons. The Southern zone, in particular, displayed impressive results in the reconstruction of Autumn temperatures, with an $R^2$ of 0.634, denoting a model that aligns well with the actual temperature changes. This is further supported by a Rel. MAE of 0.604, reinforcing the model's capability to reconstruct temperature with a good degree of precision relative to the underlying variability.

This seasonal assessment underscores the LSTM models' strengths and weaknesses in reconstructing climatic variables. While the models generally reconstruct temperature effectively, as the Southern zone demonstrates across multiple seasons, precipitation remains a more intricate variable to model. The fluctuating $R^2$ values and the Relative MAE Errors above 1 for precipitation reconstruction reveal the greater complexity and stochastic nature of precipitation patterns.

The varying performance across different seasons and zones illuminates the nuanced relationship between LSTM model predictions and the inherent variability present in the climatic data. It affirms that while LSTM models hold potential in reconstructing temperature patterns with considerable accuracy, precipitation, requires a nuanced approach and further model enhancements for better alignment with observed data.

## 3.4 Impact of Annual Forcings

In the context of assessing the impact of annual forcings on model performance, it is pertinent to mention that our ablation studies were executed leveraging the complete dataset. This enabled a comprehensive evaluation of how each environmental factor individually affects the model's ability to predict climate variability, providing insights that are instrumental for refining our model and understanding the complex dynamics of the Mediterranean climate system.

The annual assessment of climatic drivers on temperature and precipitation reconstructions provides insightful contrasts, as visually depicted in Figure 10 for temperature. The chart shows that the ablation of CO2 results in a notable deviation from the actual temperature rise, emphasizing its fundamental role in capturing the warming trend. The reconstruction without CO2 flattens the increasing temperature curve, highlighting the gas's significant contribution to recent warming trends.

Looking at the Score Differences (Figure 11, left panel), CO2 remains the primary driver in the Central Mediterranean, with a value of 0.0268, underscoring its significant impact on the warming trend. Precipitation (Figure 11, right panel) reconstructions, however, show a varying influence of CO2 across the regions, with the most substantial effect in the South Mediterranean (ScoreDifference of 0.0047), followed by the Central (0.0019) and North (0.00004) areas. This gradient may reflect regional differences in CO2's hydrological impact, from precipitation patterns to intensity.

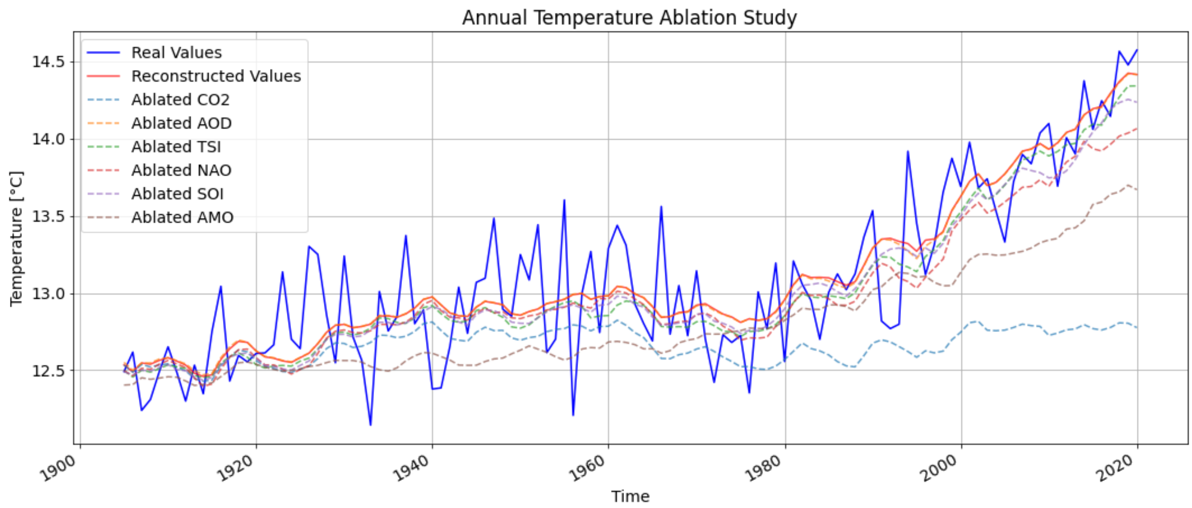


*Figure 10. Temperature Ablation Study for Central Mediterranean: This chart compares actual temperatures against model-predicted values with the successive ablation of individual climate inputs. Notably, the ablation of CO2 data results in a significant divergence from the increasing trend of actual temperatures, almost nullifying the observed warming effect. This stark contrast illustrates CO2's critical role in temperature rise and the effectiveness of the model in capturing this when CO2 is included.*

The Aerosol Optical Depth presents a contrasting effect: it has a minor influence on temperature but shows a more pronounced impact on precipitation, especially in the North Mediterranean with a ScoreDifference of 0.0014, possibly due to its role in cloud formation and albedo effects. The Atlantic Multidecadal Oscillation is another feature that exhibits divergence between temperature and precipitation. While it significantly affects temperature (with a ScoreDifference of 0.0033 in the South), it has a negative ScoreDifference for precipitation in the North and South Mediterranean, indicating a complex interplay with regional hydroclimate. However, the poor quality of the reconstruction of precipitation suggest caution in the interpretation of these results.

The North Atlantic Oscillation demonstrates modest effects across both temperature and precipitation reconstructions, with a more marked negative impact on precipitation in the South (ScoreDifference of

-0.0006). The Total Solar Irradiance and Southern Oscillation Index show marginal and sometimes negative ScoreDifferences, suggesting a subtle influence on the annual climatic patterns in the Mediterranean region.

### 3.5 Impact of Monthly and Seasonal Forcings

On a monthly scale, the ScoreDifferences for temperature (Figure 12, left side) highlight the dominance of CO2, particularly in the South Mediterranean with a striking ScoreDifference of 0.0470. Precipitation (Figure 12, right side) is also significantly influenced by CO2, especially in the Central Mediterranean (ScoreDifference of 0.0018). Notably, the Atlantic Multidecadal Oscillation shows the highest monthly ScoreDifference in the Central Mediterranean for precipitation at 0.0076, far surpassing its influence on temperature. This suggests that AMO could be a key factor in monthly precipitation variability.
Seasonally, the impact of these forcings on precipitation and temperature exhibits regional specificity (Figure 14 and Figure 15).

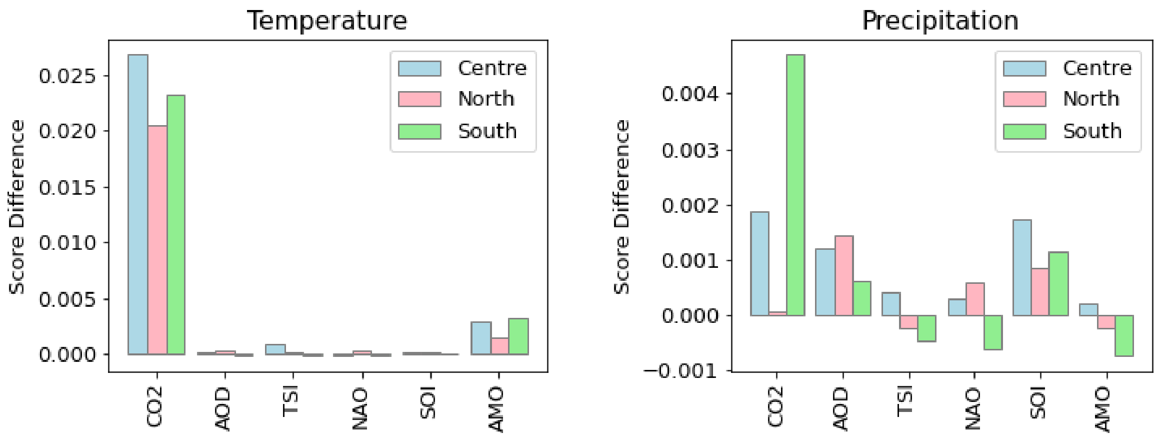


*Figure 11. Ablation study results for mean annual temperature and precipitation across three distinct Mediterranean zones. The bars indicate the score differences when specific climate features, such as CO2 and AOD levels, are excluded from the model, reflecting their relative importance in predicting regional climate variations.*

For instance, the CO2 ScoreDifference peaks in winter for precipitation in the Central Mediterranean (0.0108) and in autumn for temperature in the South (0.0123). This demonstrates the strong seasonal influence of CO2 on regional climate, particularly in terms of hydrological responses. The NAO shows a complex seasonal pattern, with a significant positive ScoreDifference in summer precipitation in the North Mediterranean (0.0021) and a negative influence on temperature in the autumn across the region.

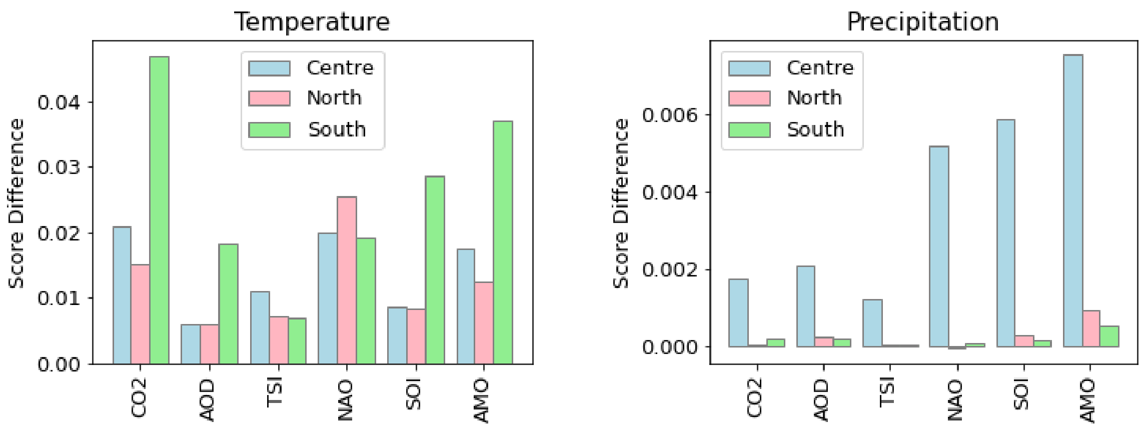


*Figure 12. Ablation study results for mean monthly temperature and precipitation across three distinct Mediterranean zones. The bars indicate the score differences when specific climate features, such as CO2 and AOD levels, are excluded from the model, reflecting their relative importance in predicting regional climate variations.*

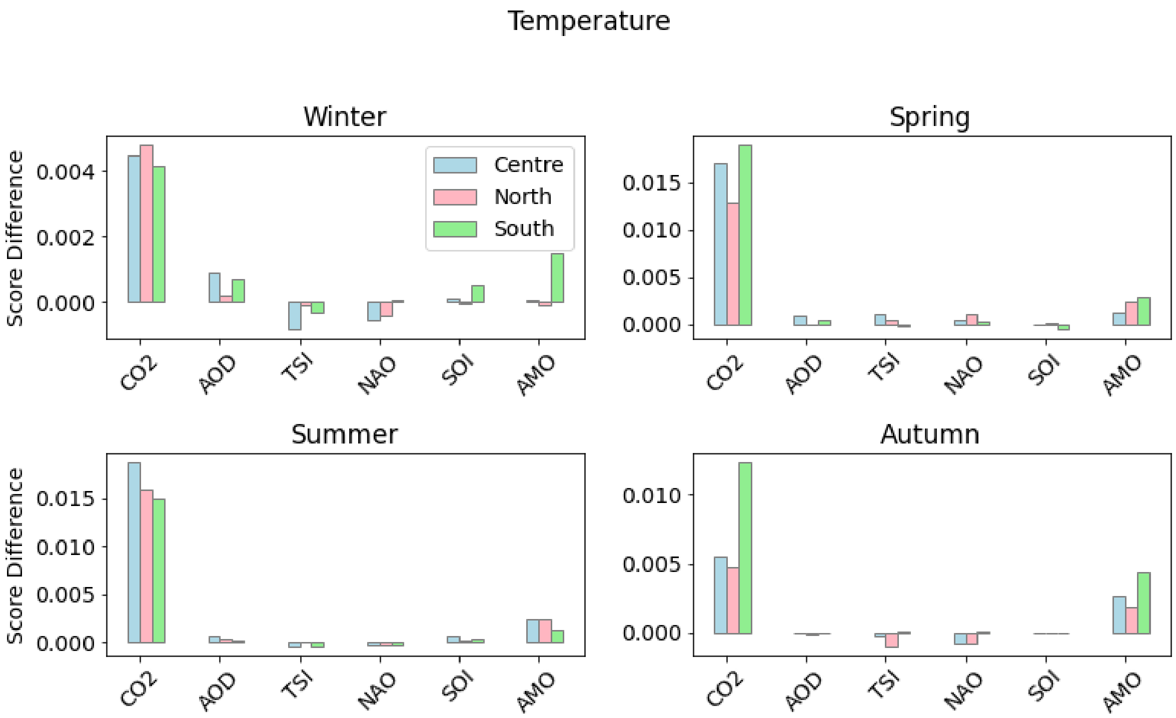


*Figure 13. Seasonal ablation study results for mean temperature across the Mediterranean's northern, central, and southern zones. Each bar represents the impact on model performance, measured by score difference, when excluding specific climate drivers for winter, spring, summer, and autumn. The chart highlights the varying importance of these drivers across different seasons, with CO2 consistently showing the largest impact, indicating its crucial role in seasonal temperature variability within the region.*

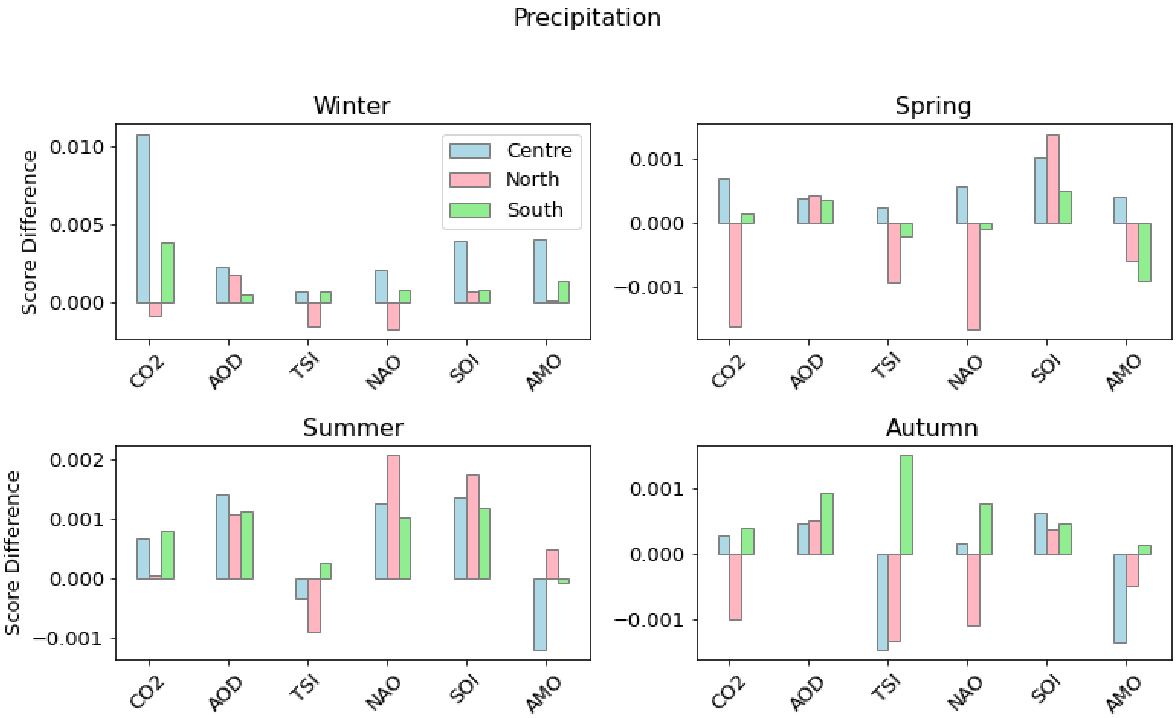


*Figure 14. Seasonal ablation study results for precipitation in the central, northern, and southern Mediterranean regions. The depicted score differences upon removal of specific climatic drivers, showcase their differential influences on predicting seasonal precipitation patterns across these zones.*

The AOD and TSI impacts are modest across the seasons, yet they present interesting patterns, such as the AOD's peak impact on winter precipitation in the North (ScoreDifference of 0.0018), possibly linked to seasonal emission variations. Meanwhile, TSI shows a negative ScoreDifference for autumn precipitation in the Central region (-0.0015), hinting at the nuanced relationship between solar radiation and seasonal weather patterns.

# 4 Conclusion

This thesis has used LSTM networks to analyse the influence of environmental forcings on climate variability of temperature and precipitation in the Mediterranean. The results underscore the primacy of $CO_2$ across all examined temporal resolutions and geographical areas for temperature reconstruction, affirming its critical role amidst anthropogenic factors in climate modeling.

The analysis has highlighted the LSTM's adeptness in modelling temperature. Notably, the ablation study revealed the nuanced impact of various forcings such as TSI, AOD, and climatic indices, emphasizing the complexity of their interactions with the regional climate system and their important role on temperature variations at monthly scale. However, it has also revealed inherent challenges in reconstructing precipitation at all time scales. This issue requires further investigations for a proper identifying the source of the model failure, which is disappointing particularly for NAO, whose role on Mediterranean precipitation is well documented in the literature.

Moving forward, this work underscores the importance of refining models by incorporating datasets that offer greater specificity and broader input variables, especially to enhance precipitation reconstruction. Precision in climate modelling relies not only on data resolution but necessitates the careful integration of complex variables influencing precipitation patterns. As the Mediterranean region continues to serve as a focal point for understanding the intricacies of climate change, this LSTMs can contribute to a foundational understanding and aid in the development of more resilient and informed climate strategies.

In closing, the integration of LSTM networks within climatological research can provide not only a deeper insight into the present climate dynamics but also opened doors for innovative approaches to forecast future conditions. This endeavor sets a precedent for future studies to build upon, potentially incorporating broader datasets, exploring alternative modeling techniques, and extending the analytical framework to include more diverse environmental forcings. The potential to refine and enhance these models is vast, and as climate science evolves, so too will the tools we use to interpret its complexities.

# References


Ali, E., W. Cramer, J. Carnicer, E. Georgopoulou, N.J.M. Hilmi, G. Le Cozannet, and P. Lionello, 2022: Cross-Chapter Paper 4: Mediterranean Region Supplementary Material. In: *Climate Change 2022: Impacts, Adaptation, and Vulnerability.* Contribution of Working Group II to the Sixth Assessment Report of the Intergovernmental Panel on Climate Change [H.-O. Pörtner, D.C. Roberts, M. Tignor, E.S. Poloczanska, K. Mintenbeck, A. Alegría, M. Craig, S. Langsdorf, S. Löschke, V. Möller, A. Okem, B. Rama (eds.)].

Allan, R. J., Nicholls, N., Jones, P. D., & Butterworth, I. J. (1991). A further extension of the Tahiti-Darwin SOI, early ENSO events and Darwin pressure. *Journal of Climate*, *4*(7), 743-749.

Compo, G. P., Whitaker, J. S., Sardeshmukh, P. D., Matsui, N., Allan, R. J., Yin, X., ... & Worley, S. J. (2011). The twentieth century reanalysis project. *Quarterly Journal of the Royal Meteorological Society*, *137*(654), 1-28.

Cherif, S., Doblas-Miranda, E., Lionello, P., Borrego, C., Giorgi, F., Rilov, G., ... & Zittis, G. (2020). Drivers of change. Climate and Environmental Change in the Mediterranean Basin–Current Situation and Risks for the Future. First Mediterranean Assessment Report, 59-180.

Emmert-Streib, F., Yang, Z., Feng, H., Tripathi, S., & Dehmer, M. (2020). An introductory review of deep learning for prediction models with big data. *Frontiers in Artificial Intelligence*, *3*, 4.

Enfield, D. B., Mestas-Nuñez, A. M., & Trimble, P. J. (2001). The Atlantic multidecadal oscillation and its relation to rainfall and river flows in the continental US. *Geophysical research letters*, *28*(10), 2077-2080.

Hamidi, M., & Roshani, A. (2023). Investigation of climate change effects on Iraq dust activity using LSTM. *Atmospheric Pollution Research*, *14*(10), 101874.

Harris, I., Osborn, T. J., Jones, P., & Lister, D. (2020). Version 4 of the CRU TS monthly high-resolution gridded multivariate climate dataset. *Scientific data*, *7*(1), 109.

Hou, S., Li, W., Liu, T., Zhou, S., Guan, J., Qin, R., & Wang, Z. (2021). D2CL: A dense dilated convolutional LSTM model for sea surface temperature prediction. *IEEE Journal of Selected Topics in Applied Earth Observations and Remote Sensing*, *14*, 12514-12523.

Lean, J., Beer, J., & Bradley, R. (1995). Reconstruction of solar irradiance since 1610: Implications for climate change. *Geophysical Research Letters*, *22*(23), 3195-3198.

Li, Q., Zhu, Y., Shangguan, W., Wang, X., Li, L., & Yu, F. (2022). An attention-aware LSTM model for soil moisture and soil temperature prediction. *Geoderma*, *409*, 115651.

Li, X., & Hsu, P.-C. (2020). Forecasting Climatic Trends Using Neural Networks: An Experimental Study Using Global Historical Data. *Frontiers in Environmental Science, 8*. https://doi.org/10.3389/fenvs.2020.00002

Lionello, P., & Scarascia, L. (2018). The relation between climate change in the Mediterranean region and global warming. *Regional Environmental Change*, *18*, 1481-1493.

Lionello, P., Malanotte-Rizzoli, P., Alpert, P., Artale, V., Boscolo, R., Garcia-Herrera, R., ... & Ulbrich, U. (2006). MEDCLIVAR: Mediterranean CLImate VARiability and predictability project. *PAGES News/CLIVAR Exchanges*, *13*, 3-5.

Lionello, P. (Ed.). (2012). The climate of the Mediterranean region: From the past to the future. Elsevier.

Pappas, C., & Athanasiadis, I. N. (2021). Harnessing deep learning to forecast local microclimate using global climate data. *Scientific Reports*, *11*(1), 12345. https://doi.org/10.1038/s41598-021-85654-3

Pasini, A., Lorè, M., & Ameli, F. (2006). Neural network modelling for the analysis of forcings/temperatures relationships at different scales in the climate system. Ecological Modelling, 191(1), 58-67.

Pasini, A., Racca, P., Amendola, S., Cartocci, G., & Cassardo, C. (2017). Attribution of recent temperature behaviour reassessed by a neural-network method. *Scientific reports*, *7*(1), 17681.

Ropelewski, C. F., & Jones, P. D. (1987). An extension of the Tahiti–Darwin southern oscillation index. *Monthly weather review*, *115*(9), 2161-2165.

Sato, M., Hansen, J. E., McCormick, M. P., & Pollack, J. B. (1993). Stratospheric aerosol optical depths, 1850–1990. *Journal of Geophysical Research: Atmospheres*, *98*(D12), 22987-22994.

Schneider, Udo; Hänsel, Stephanie; Finger, Peter; Rustemeier, Elke; Ziese, Markus (2022): GPCC Full Data Monthly Product Version 2022 at 0.5°: Monthly Land-Surface Precipitation from Rain-Gauges built on GTS-based and Historical Data. DOI: 10.5676/DWD_GPCC/FD_M_V2022_050

Wei, Y., S. Liu, D.N. Huntzinger, A.M. Michalak, N. Viovy, W.M. Post, C.R. Schwalm, K. Schaefer, A.R. Jacobson, C. Lu, H. Tian, D.M. Ricciuto, R.B. Cook, J. Mao, and X. Shi. (2014). NACP MsTMIP: Global and North American Driver Data for Multi-Model Intercomparison. Data set. Available on-line [http://daac.ornl.gov] from Oak Ridge National Laboratory Distributed Active Archive Center, Oak Ridge, Tennessee, USA. http://dx.doi.org/10.3334/ORNLDAAC/1220

Zhang, K., Geng, X., & Yan, X. H. (2020). Prediction of 3-D ocean temperature by multilayer convolutional LSTM. *IEEE Geoscience and Remote Sensing Letters*, *17*(8), 1303-1307.

## A. APPENDIX: Evaluation tables

| Area | Metric | Annual | Monthly | Winter | Spring | Summer | Autumn |
|---|---|---|---|---|---|---|---|
| North | $R^2$ | 0.562 | 0.912 | 0.120 | 0.264 | 0.111 | 0.189 |
| | Rel. MAE | 0.770 | 0.262 | 0.980 | 0.905 | 0.914 | 0.824 |
| Centre | $R^2$ | 0.529 | 0.954 | 0.052 | 0.176 | 0.308 | 0.183 |
| | Rel. MAE | 0.710 | 0.187 | 0.943 | 0.818 | 0.771 | 0.861 |
| South | $R^2$ | 0.681 | 0.961 | -0.084 | 0.489 | 0.447 | 0.627 |
| | Rel. MAE | 0.594 | 0.167 | 0.999 | 0.687 | 0.753 | 0.617 |

*Table 1. Comparative Performance Metrics of LSTM Models for Temperature Reconstruction. This table summarizes the coefficient of determination ($R^2$) and Relative Mean Absolute Error (Rel. MAE) for annual, monthly, and seasonal temperature reconstructions across the Northern, Central, and Southern Mediterranean regions.*

| Area | Metric | Annual | Monthly | Winter | Spring | Summer | Autumn |
|---|---|---|---|---|---|---|---|
| North | $R^2$ | -0.048 | -0.032 | -0.240 | -0.208 | -0.039 | -0.250 |
| | Rel. MAE | 0.823 | 1.006 | 1.027 | 1.108 | 0.996 | 1.136 |
| Centre | $R^2$ | -0.068 | 0.433 | 0.094 | -0.241 | -0.129 | -0.175 |
| | Rel. MAE | 0.847 | 0.693 | 0.945 | 1.160 | 1.083 | 1.075 |
| South | $R^2$ | -1.016 | -0.004 | 0.296 | -0.154 | 0.002 | -0.286 |
| | Rel. MAE | 0.794 | 0.996 | 0.868 | 1.101 | 1.013 | 1.161 |

*Table 2. Performance Evaluation of LSTM Models for Precipitation Reconstruction. Displayed here are the $R^2$ and Rel. MAE values reflecting the models' predictive accuracy for annual, monthly, and by-season precipitation data, segmented by the Northern, Central, and Southern zones of the Mediterranean.*

| Area | Feature | Annual | Monthly | Winter | Spring | Summer | Autumn |
|---|---|---|---|---|---|---|---|
| Nord | $CO_2$ | 0.02049 | 0.01520 | 0.00478 | 0.01284 | 0.01593 | 0.00473 |
| | AOD | 0.00031 | 0.00592 | 0.00021 | -0.00012 | 0.00025 | -0.00015 |
| | TSI | 0.00013 | 0.00722 | -0.00010 | 0.00052 | -0.00005 | -0.00096 |
| | NAO | 0.00039 | 0.02560 | -0.00040 | 0.00112 | -0.00024 | -0.00072 |
| | SOI | 0.00014 | 0.00829 | -0.00004 | 0.00015 | 0.00010 | 0.00000 |
| | AMO | 0.00147 | 0.01243 | -0.00009 | 0.00235 | 0.00239 | 0.00188 |
| Centre | $CO_2$ | 0.02680 | 0.02103 | 0.00447 | 0.01698 | 0.01873 | 0.00551 |
| | AOD | 0.00020 | 0.00606 | 0.00088 | 0.00092 | 0.00064 | -0.00000 |
| | TSI | 0.00087 | 0.01099 | -0.00082 | 0.00106 | -0.00042 | -0.00018 |
| | NAO | -0.00006 | 0.02007 | -0.00054 | 0.00043 | -0.00034 | -0.00074 |
| | SOI | 0.00018 | 0.00862 | 0.00010 | 0.00004 | 0.00058 | 0.00004 |
| | AMO | 0.00295 | 0.01745 | 0.00006 | 0.00130 | 0.00239 | 0.00266 |
| South | $CO_2$ | 0.02322 | 0.04701 | 0.00414 | 0.01890 | 0.01500 | 0.01230 |
| | AOD | -0.00003 | 0.01827 | 0.00069 | 0.00050 | 0.00019 | 0.00002 |
| | TSI | -0.00008 | 0.00700 | -0.00031 | -0.00020 | -0.00040 | 0.00009 |
| | NAO | -0.00015 | 0.01917 | 0.00004 | 0.00033 | -0.00035 | 0.00011 |
| | SOI | 0.00005 | 0.02873 | 0.00053 | -0.00052 | 0.00029 | 0.00000 |
| | AMO | 0.00331 | 0.03719 | 0.00152 | 0.00283 | 0.00128 | 0.00443 |

*Table 3. Ablation Study Scores for Temperature Reconstruction Models Across Mediterranean Regions. This table outlines the influence of individual climatic features on the annual, monthly, and seasonal temperature by presenting the score differences when each feature is excluded from the LSTM models.*

| Area | Feature | Annual | Monthly | Winter | Spring | Summer | Autumn |
|---|---|---|---|---|---|---|---|
| Nord | CO2 | 0.00004 | 0.00005 | -0.00089 | -0.00161 | 0.00006 | -0.00100 |
| | AOD | 0.00143 | 0.00025 | 0.00177 | 0.00043 | 0.00106 | 0.00052 |
| | TSI | -0.00024 | 0.00004 | -0.00154 | -0.00093 | -0.00089 | -0.00133 |
| | NAO | 0.00058 | -0.00007 | -0.00170 | -0.00166 | 0.00207 | -0.00108 |
| | SOI | 0.00086 | 0.00026 | 0.00069 | 0.00139 | 0.00174 | 0.00038 |
| | AMO | -0.00023 | 0.00092 | 0.00012 | -0.00060 | 0.00048 | -0.00049 |
| Centre | CO2 | 0.00187 | 0.00177 | 0.01084 | 0.00069 | 0.00065 | 0.00029 |
| | AOD | 0.00118 | 0.00208 | 0.00224 | 0.00039 | 0.00139 | 0.00047 |
| | TSI | 0.00040 | 0.00121 | 0.00071 | 0.00024 | -0.00034 | -0.00146 |
| | NAO | 0.00029 | 0.00521 | 0.00208 | 0.00057 | 0.00124 | 0.00018 |
| | SOI | 0.00173 | 0.00591 | 0.00397 | 0.00103 | 0.00136 | 0.00064 |
| | AMO | 0.00021 | 0.00756 | 0.00403 | 0.00040 | -0.00120 | -0.00135 |
| South | CO2 | 0.00471 | 0.00021 | 0.00388 | 0.00014 | 0.00079 | 0.00041 |
| | AOD | 0.00060 | 0.00020 | 0.00047 | 0.00036 | 0.00111 | 0.00092 |
| | TSI | -0.00048 | 0.00005 | 0.00067 | -0.00020 | 0.00025 | 0.00152 |
| | NAO | -0.00061 | 0.00007 | 0.00076 | -0.00008 | 0.00101 | 0.00076 |
| | SOI | 0.00113 | 0.00015 | 0.00082 | 0.00050 | 0.00116 | 0.00046 |
| | AMO | -0.00076 | 0.00054 | 0.00138 | -0.00092 | -0.00008 | 0.00014 |

*Table 4. Ablation Study Results for Precipitation Reconstruction Models in the Mediterranean Zones. Detailed here are the score differences for annual, monthly, and seasonal, illustrating the impact of removing specific climatic drivers on the LSTM models' accuracy in precipitation forecasting.*